JOC The Journal of Organic Chemistry

pubs.acs.org/joc Article

Role of Acetate Anions in the Catalytic Formation of Isocyanurates from Aromatic Isocyanates

Yunfei Guo,[⊥] Mikko Muuronen,*[,⊥] Peter Deglmann, Frederic Lucas, Rint P. Sijbesma, and Željko Tomović*

Cite This: J. Org. Chem. 2021, 86, 5651−5659 Read Online

ACCESS | Metrics & More | Article Recommendations | Supporting Information

ABSTRACT: The formation of isocyanurates via cyclotrimerization of aromatic isocyanates is widely used to enhance the physical properties of a variety of polyurethanes. The most commonly used catalysts in industries are carboxylates for which the exact catalytically active species have remained controversial. We investigated how acetate and other carboxylates react with aromatic isocyanates in a stepwise manner and identified that the carboxylates are only precatalysts in the reaction. The reaction of carboxylates with an excess of aromatic isocyanates leads to irreversible formation of corresponding deprotonated amide species that are strongly nucleophilic and basic. As a result, they are active catalysts during the nucleophilic anionic trimerization, but can also deprotonate urethane and urea species present, which in turn catalyze the isocyanurate formation. The current study also shows how quantum chemical calculations can be used to direct spectroscopic identification of reactive intermediates formed during the active catalytic cycle with predictive accuracy.

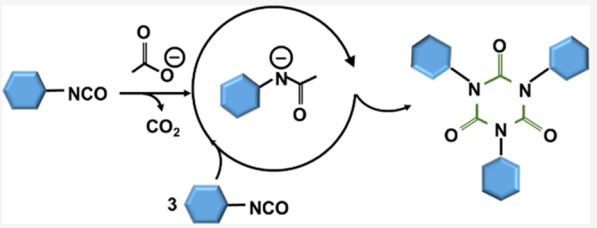

1. INTRODUCTION

Isocyanurates, heterocyclic structures of 1,3,5-triazine-2,4,6-trione, formed via cyclotrimerization of isocyanates are widely used to enhance the physical properties of a variety of polyurethanes.[1−4] Whereas the controlled trimerization of aliphatic isocyanates is used for the preparation of isocyanurate cross-linkers for high-performance polyurethane coatings,[5−8] the cyclotrimerization of aromatic isocyanates into polyisocyanurate (PIR) structures is used to improve the thermal stability and flame retardancy of polyurethane rigid foams.[9−17] The initial molar ratio of functional groups and especially the type of catalyst are the main factors influencing the formation of PIR structures. The most commonly used catalysts in industrial applications are based on carboxylates, such as potassium acetate, potassium 2-ethylhexanoate, trimethyl hydroxypropyl ammonium formate, or phenolate such as 2,4,6-tris-(dimethylaminomethyl)phenol.[6,18−25] The various industrial and commercial applications of isocyanurate-based polyurethane materials have attracted much attention in developing more effective catalysts for isocyanate trimerization. A number of catalysts for the trimerization of isocyanates have been extensively studied and reported in academic literature, including among others tetrabutylammonium fluoride (TBAF),[26] 2-phosphaethynolate anion (OCP^-),[27] sodium *p*-toluenesulfinate (*p*-TolSO$_2$Na)/tetrabutylammonium iodide (TBAI),[28,29] tetrakis(dimethylamino)ethylene (TDAE),[30] proazaphosphatrane,[31−33] N-heterocyclic carbenes, olefins,[34,35] etc. With more and more catalysts being reported, the exact nature of the cyclotrimerization mechanism has raised much interest.

The generally accepted mechanism for the anionic trimerization of aromatic isocyanates is shown in Scheme 1. In this mechanism, the nucleophilic anionic catalyst (**1**) adds to the isocyanate carbon forming a nucleophilic anionic intermediate **2**, which reacts further in the presence of excess isocyanate to form the trimeric isocyanurates (**6**).[26,28,32,34,36] In the case of industrially used acetate-based catalysts, however, the exact nature of the catalytic species is controversial. Most studies consider the catalytically active species to be the acetate anion itself,[37,38] but, on the other hand, Hoffman's early experimental work indicated that acetate anions are quickly converted to acetanilide when reacting with aromatic isocyanates, which in turn could potentially act as the anionic catalysts in the active cycle.[39] Further, as the acetanilide anion can be expected to deprotonate urethane, allophanate, urea, and biuret groups in the PU matrix depending on their relative acidities, and their corresponding anions have been shown to be active PIR catalysts, the catalytically active species is expected to change several times during the polymerization.[13,19,40] Recently, Siebert et al. also

Received: January 15, 2021
Published: April 1, 2021

https://doi.org/10.1021/acs.joc.1c00119
J. Org. Chem. 2021, 86, 5651−5659

Scheme 1. Generally Accepted Anionic Trimerization Mechanism of Aromatic Isocyanates

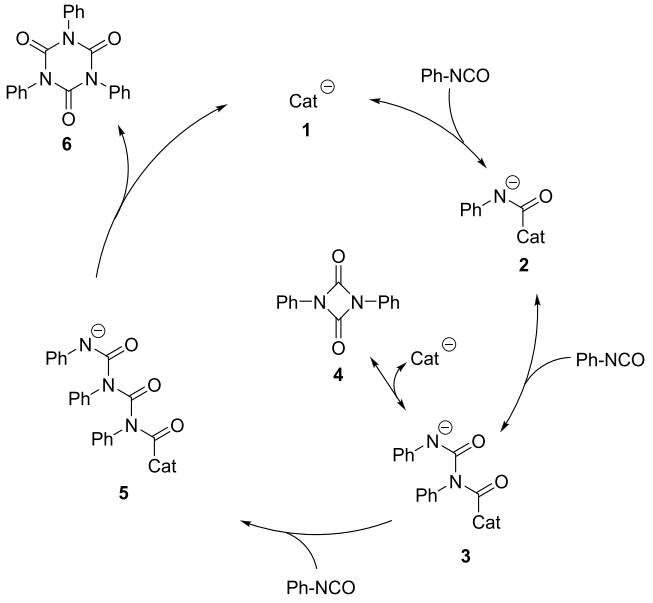

suggested that the catalytically active species originating from acetate anions changes several times during the cyclotrimerization of aliphatic isocyanates.[41] The exact species that catalyze cyclotrimerization of aromatic isocyanates, however, has not been explicitly characterized so far, which hampers the development of new PIR catalysts suitable for large-scale polyurethane production.

Here, we study the role of acetate anions in the cyclotrimerization of aromatic isocyanates. Our study is based on first using the state-of-the-art quantum chemical methods to investigate how the acetate anion reacts with aromatic isocyanates in a stepwise manner to identify plausible mechanistic pathways. These are then used to guide spectroscopic identification of the catalytically active species to confirm the predicted mechanistic pathways.

2. RESULTS AND DISCUSSION

We studied the cyclotrimerization of aromatic isocyanates using phenyl and *p*-tolyl isocyanates as model substrates for identifying the species that are formed when acetate anion reacts with an excess of aromatic isocyanates (see Scheme 2). First, we calculated the relative free energies for several plausible mechanistic pathways for acetate anion-catalyzed cyclotrimerization of phenyl isocyanate in toluene and tetrahydrofuran (THF). Calculations were performed using accurate quantum chemical methods, i.e., all structures were optimized using dispersion-corrected density functional theory, namely the TPSS-D3[42,43] functional with triple-ζ def2-TZVP[44,45] basis sets, and the final relative free energies were calculated using resolution-of-identity random phase approximation (RIRPA)[46] with quadruple-ζ def2-QZVPP basis sets in toluene and tetrahydrofuran (THF) as described in the experimental section. The accuracy of the used methods has been recently discussed elsewhere and is thus not addressed here.[47−49] These data were then used to understand which intermediates are formed during the active catalytic cycle for guiding their experimental identification directly from the reaction mixture using liquid chromatography−mass spectrometry (LC−MS) and $^{1}H-^{13}C$ heteronuclear single quantum coherence (HSQC) nuclear magnetic resonance (NMR) spectroscopy. In the experiments in toluene and THF, catalyst loading of 10 mol % relative to isocyanate was used to ensure that the ionic intermediates are formed in high enough concentrations to be detected with the analytical methods used (see Section 4 and the Supporting Information for full details on computational and experimental methods).

Scheme 2. Model Reaction for Studying the Catalyzed Trimerization of Aromatic Isocyanates

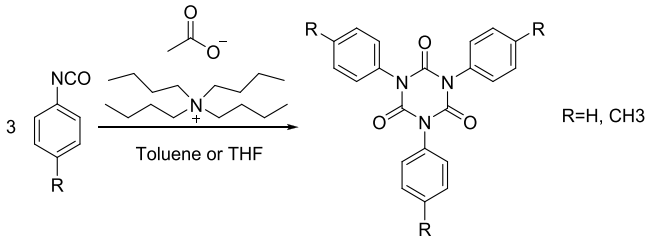

The calculated mechanistic pathways in THF and their corresponding relative free energies are shown in Figure 1 (for results in toluene, see Tables S1 and S2). In the generally accepted reaction mechanism, acetate anions react in a stepwise manner with 3 equiv of isocyanates to form isocyanurate (**6**) (see Figure 1a,b). The reaction is initiated by straightforward nucleophilic addition of an acetate anion (**1**) to aromatic isocyanate forming an acetate bound isocyanate complex **2**. This nucleophilic intermediate can then react with the second isocyanate to form an allophanate acetate complex **3** that can reversibly cyclize intramolecularly to form 1,3-diphenyl-2,4-uretidinedione (**4**) as the kinetic product or react with the third isocyanate to form intermediate **5**, leading to the formation of isocyanurate **6** via its catalyst bound intermediate **6-cat** as the thermodynamic product. Overall, the reaction is strongly exergonic and the calculated low activation free energies agree well with the experimentally observed fast reaction at room temperature, i.e., the rate-limiting activation free energies are 65 and 67 kJ/mol in THF and toluene, respectively (**1** → **TS3-5**).

However, while the straightforward mechanism is energetically plausible, we do not consider this mechanism to be the active catalytic cycle, as the allophanate acetate intermediate **3** is predicted to react intramolecularly with lower activation free energy to form intermediate **3b** via acetyl migration instead of reacting intermolecularly with isocyanate to form the intermediate **5**. After the elimination of CO_2, the intramolecular pathway is expected to form intermediate **2′** irreversibly, a product of deprotonated amide and isocyanate. The amide could also be formed directly from intermediate **2** via a four-membered transition state **TS2-2b**: the free energy difference between transition states **TS2-2b** and **TS2-3** is calculated to be only 12 kJ/mol, indicating that both pathways are plausible or can even coexist.

The formed deprotonated aromatic amide **1′** is nucleophilic and reacts with excess isocyanates to form isocyanurate **6** identically to the previously explained catalytic cycle as shown in Figure 1. Both catalytic cycles are also energetically very similar with activation free energies of 61 and 60 kJ/mol in THF and toluene, respectively (**3′** → **TS3′-5′**). While in the catalytic cycle on the right, the active species cannot undergo similar catalyst migrations as previously, the allophanate isocyanate intermediate **3′** is interestingly predicted to

https://doi.org/10.1021/acs.joc.1c00119
J. Org. Chem. 2021, 86, 5651−5659

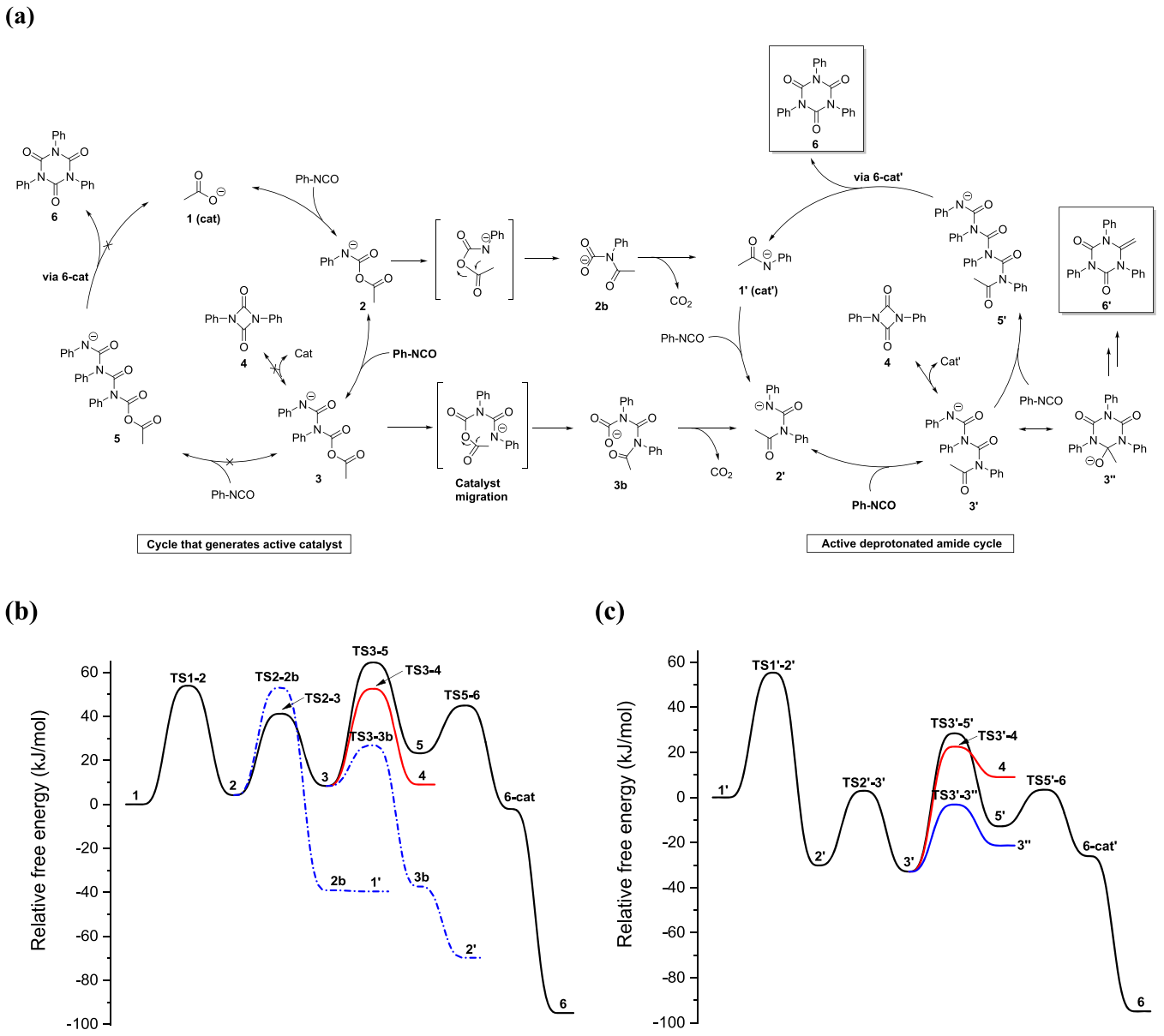

Figure 1. Reaction mechanism and the relative free energies (in kJ/mol) for the studied reaction mechanisms. All relative free energies are calculated in THF at 25 °C (see Tables S1 and S2 for numerical values).

reversibly form the cyclized anion **3″**, which we consider to lead to the formation of electron-poor N-heterocyclic olefin **6′** in agreement with recent findings in the cyclotrimerization of aliphatic isocyanates.[41] The total reaction yields one molar equivalent of hydroxyl anions, but we assume the reaction to proceed via first protonating **3′** by a trace amount of proton sources and then fragmenting water. Water and hydroxyl anions are well known to lead to the formation of urea first by hydrolyzing isocyanate to carbamic acid and forming an aromatic amine after fragmentation of CO_2.[50] The formed aromatic amine reacts with the second isocyanate equivalent to form urea, which under basic conditions can be deprotonated to form a new anionic catalyst similar to **1′**. Therefore, forming olefin **6′** does not end the catalytic isocyanurate formation, but instead changes the catalytically active species from the deprotonated amide to deprotonated urea in agreement with findings for aliphatic isocyanates.[41]

Then, we studied the trimerization reaction experimentally in THF and toluene at room temperature to verify our mechanistic hypothesis. For experiments, we chose phenyl and *p*-tolyl isocyanates as model substrates and tetrabutylammonium acetate (TBAA) as catalyst because of their high solubility in both solvents. The reaction was monitored using Fourier-transform infrared spectroscopy (FTIR) and once all isocyanates had reacted, the mixture was analyzed using liquid chromatography−mass spectrometry (LC−MS) to detect the reactive intermediates present in the solution (see Table 1 and Figure 2). The observed signals agree completely with the mechanism depicted in Figure 1a, being exclusively associated with the deprotonated amide cycle, product **6**, olefinic product **6′**, and urea (see Table 1). Results were independent of the substrate (phenyl or *p*-tolyl isocyanate) or of the solvent (THF or toluene). Therefore, only results from experiments with phenyl isocyanate in THF are discussed below unless

https://doi.org/10.1021/acs.joc.1c00119
J. Org. Chem. 2021, 86, 5651−5659

Table 1. High Abundance Signals Observed from the Positive-Ion Mode of LC−MS Analysis of the Product After Cyclotrimerization of Phenyl Isocyanate with TBAA in Dry THF

m/z	Abundance (%)	Assignment	m/z	Abundance (%)	Assignment
136.00	2	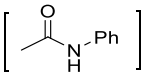	332.08	14	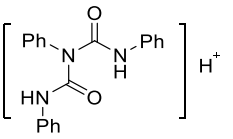
213.08	9	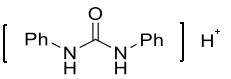	356.17	31	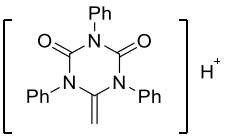
242.25	100	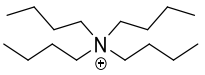	358.17	40	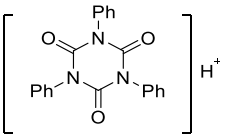
255.00	7	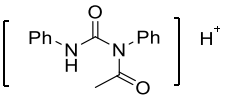	396.00	26	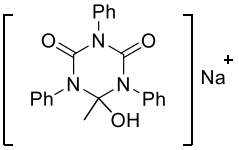 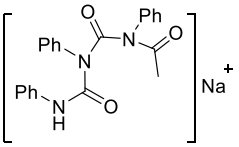

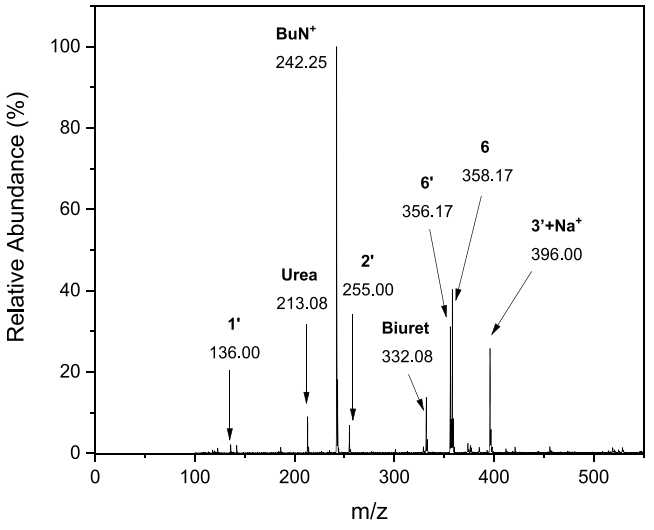

Figure 2. LC−MS spectra after reaction of phenyl isocyanate and 10 mol % TBAA in dry THF and evaporation of the solvent.

otherwise noted. Additional experimental data are found in the Supporting Information.

The calculated relative free energies of the reactive intermediates indicate that we should be able to detect intermediates **1′**, **2′**, and **3′** but not intermediate **5′** due to its higher relative free energy and fast cyclization to form product **6**. The intermediates **1′** and **2′** are observed in their protonated forms with signals m/z = 136.00, m/z = 255.00, but at the same time intermediate **3′** in its protonated form at m/z = 374.15 is too weak to be conclusively analyzed although it is predicted to be thermodynamically more stable than intermediate **2′** (see Figure 1c). The rationale for the absence of a peak at m/z = 374.15 is that intermediate **3′** is actually found at m/z = 396.00 as a complex with one sodium cation. Intermediate **3′** was also detected as dimer coordinating to one sodium cation (see the Supporting Information for further discussion, Figure S1).

We observed two signals associated with the products: protonated triphenyl isocyanurate (**6**) was detected at m/z = 358.17 and the protonated "olefinic isocyanurate" **6′** was found at m/z = 356.17. The formation of **6′** was also confirmed by the presence of NMR signals of olefinic CH_2 protons at 3.01 ppm and the associated sp^2 carbon signal at 75.6 ppm using $^1H-^{13}C$-HSQC spectroscopy (see Figure 3). Detection of urea at m/z = 213.08 and biuret at m/z = 332.08 also supports the hypothesis that the eliminated water starts a new catalytic cycle with deprotonated urea as the catalytically active species although trace amounts of water could also have been present as impurities. When *p*-tolyl isocyanate was used as a trimerization starting material, the corresponding isocyanurate **6** was detected as a dimer with one sodium cation at m/z = 820.83 (Figure S3). This assignment was also confirmed by finding the same signal in a purified sample of tris-*p*-tolyl-isocyanurate **6** in LC−MS (Figure S5), which can be rationalized by the strong tendency of isocyanurate rings to form supramolecular dimers as simulated by Lenzi et al.[51]

Finally, to verify that deprotonated amides catalyze the reaction, we performed the same reaction using commercially available acetanilide as a catalyst deprotonated in situ by excess triethylamine. The reaction was significantly slower due to the

https://doi.org/10.1021/acs.joc.1c00119
J. Org. Chem. 2021, 86, 5651−5659

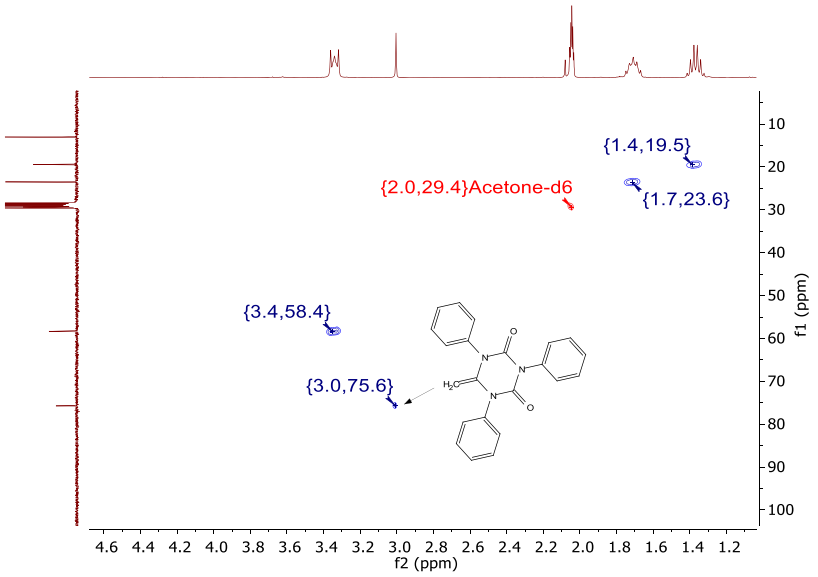

Figure 3. $^{1}H-^{13}C$ HSQC spectrum in acetone-d_6 after reaction of phenyl isocyanate and 10 mol % TBAA in dry THF and evaporation of the solvent. The peak at ^{1}H—3.0 ppm, ^{13}C—75.6 ppm is assigned to the terminal CH_2 of the olefin structure.

Scheme 3. Identified Catalytically Active Species for Different Carboxylate Anions

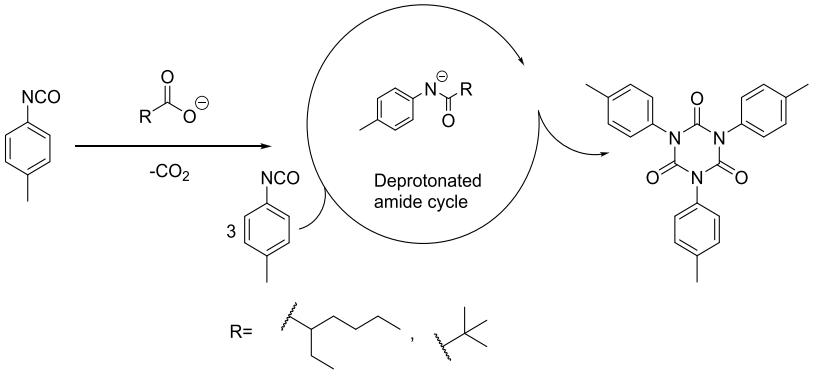

Scheme 4. Calculated Free Energies for Proton Transfers between Deprotonated Amide, Acetate, Urethane, and Urea Species in Toluene, THF, and Water[a]

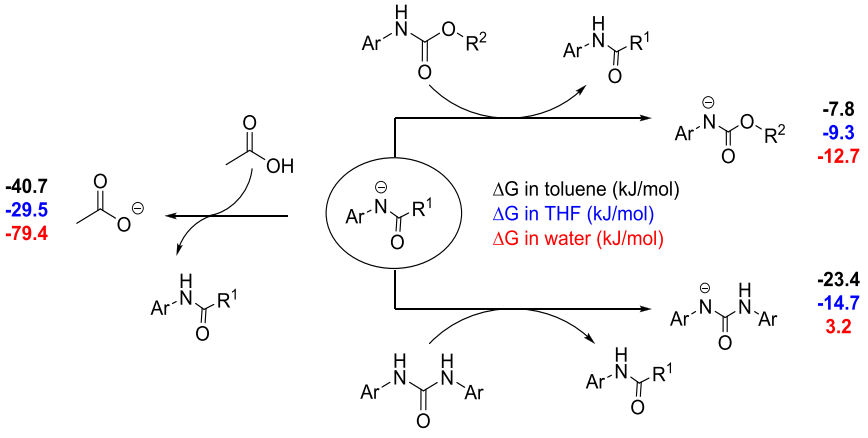

[a]All free energies are in kJ/mol and calculated for species with Ar = Ph, $R^1 = R^2$ = Me.

unfavorable deprotonation of the amide in toluene and THF, but isocyanurate product **6** was still observed in LC−MS despite the low conversion. Catalysis by deprotonated amides is also supported by early work done by Kogon, who reported the formation of aromatic isocyanate trimers in high yield at elevated temperatures when phenyl isocyanates were trimerized in the presence of *N*-methylmorpholine and ethyl alcohol or ethyl carbanilate.[13]

To understand how general the observed catalyst migration mechanism is when carboxylates are used as catalysts, we also

https://doi.org/10.1021/acs.joc.1c00119
J. Org. Chem. 2021, 86, 5651−5659

performed trimerization of *p*-tolyl isocyanate using potassium 2-ethylhexanoate at room temperature and cesium pivalate at 60 °C as the (pre)catalysts in THF (see Scheme 3). As expected, only intermediates related to the deprotonated amide cycle were found, indicating that the conversion of carboxylates into amides with aromatic isocyanates is general rather than restricted to only sterically small carboxylates such as acetate (Figures S6 and S7). For these two precatalysts, 2-ethylhexanoate could, in principle, also form an olefinic isocyanurate structure similar to **6′** via deprotonation of the tertiary α-proton, but this was not observed in our experiment.

Finally, we considered the role of the deprotonated amide cycle in catalyzing the trimerization of aromatic isocyanates during the formation of real PU materials. In these cases, several functional groups, i.e., alcohols, water, urethanes, urea, allophanates, and biurets, are present that are in deprotonation equilibrium with amide. To establish their roles, we calculated the reaction free energies for proton transfers between acetate, amide, urethane and urea (see Scheme 4). The calculations were performed in toluene and THF to understand how the polarity of the reaction media affects the relative stability of the corresponding anions, and in water as a model for a polar protic environment. In all media, the aromatic amide anion is predicted to deprotonate aromatic urethane with exergonic free energies between −7 and −13 kJ/mol, while deprotonation of urea is more dependent on the reaction media that is exergonic in toluene and THF (−23 and −15 kJ/mol, respectively), but endergonic in water (+3 kJ/mol). As expected, acetate itself is calculated to be much less basic than the deprotonated amide and direct deprotonation of urethane by acetate is calculated to be endergonic by 20−67 kJ/mol depending on the solvent. Therefore, acetate anions form amides and CO_2 with isocyanates, independent of the reaction media, but the amide anion may in turn deprotonate urethanes, urea, allophanates, or biurets present, forming new catalytically active anions that are expected to catalyze trimerization in a cycle, which is similar to that of the deprotonated amide. This is supported also by a kinetic study by Schwetlick and Noack,[40] who measured trimerization kinetics of phenyl isocyanate in acetonitrile at 50 °C using tetramethylammonium octanoate as a catalyst in the presence of several X−H active additives such as alcohols, carbamates, phenols, and amides. The measured kinetics showed that additives change the rate of isocyanurate formation significantly, confirming our hypothesis that the role of carboxylate precatalyst is twofold: first, it generates a strong base out of a weak base by reacting with aromatic isocyanate to generate a deprotonated amide, a reaction that is thermodynamically facilitated by the favorable entropy of the decarboxylation reaction. Second, the amide anion can then catalyze the PIR formation via the nucleophilic mechanism of Scheme 1, but the basic deprotonated amide can also deprotonate functional groups such as urethane and urea groups, which in turn will catalyze the anionic trimerization.

3. CONCLUSIONS

We investigated the role of acetate anions in the trimerization of aromatic isocyanates by the state-of-the-art experimental and computational methods. Our study reveals that during the anionic cyclotrimerization, the actual catalytically active species changes at least once with the acetate anion only serving as a precatalyst. The reaction of acetate anion with an excess of aromatic isocyanates leads eventually to irreversible formation of deprotonated amide species that are formed after intramolecular rearrangement and decarboxylation. The deprotonated amide is the new active catalyst that forms isocyanurate via a nucleophilic anionic mechanism. The deprotonated amides are much more basic than the acetate precatalyst and, therefore, are capable of deprotonating other protic groups in the system such as urethane and urea groups, which in turn catalyze isocyanurate formation. Carboxylate migration to amide anions is expected to take place regardless of the size of the carboxylate because migration was observed for acetate, 2-ethylhexanoate, and pivalate alike. Acetate, on the other hand, can also lead to the formation of an electron-poor N-heterocyclic olefin and water, which can further lead to a catalytic cycle where deprotonated urea is the active catalytic species. We demonstrated that the qualitative mechanism is independent of the solvent polarity. However, the effect that changes in acid−base equilibrium in protic solvents may have on the mechanism is the subject of further studies. The current study also highlights that mechanistic investigations can greatly be accelerated when using a combination of the state-of-the-art computational and experimental analytic techniques, and importantly discover details that may not be analyzed by either of the methods alone.

4. EXPERIMENTAL SECTION

4.1. Computational Details. All computations were performed using Turbomole 7.3 program package.[52] Structures were optimized using dispersion-corrected TPSS-D3[42,43] density functional with def2-TZVP[44,45] basis sets and by employing multipole-accelerated resolution-of-the-identity approximation for Coulomb term (MARI-J)[53] with the corresponding auxiliary basis sets to speed up the computations.[54] The final energy of each structure was calculated using resolution-of-identity random phase approximation (RIRPA)[46] with def2-QZVPP basis sets and with corresponding auxiliary basis sets.[55,56] RPA calculations were performed using gas-phase TPSS orbitals, and the core orbitals were kept frozen for computing the RPA correlation energy. Default settings and convergence criteria of Turbomole were used in all optimizations except a finer integration grid of *m4* was used. In RPA calculations, grid *m5* and a higher threshold for energy convergence (scfconv 7) were used for calculating the TPSS orbitals. Harmonic vibrational frequencies were calculated numerically at the level of optimization for all optimized structures.

Solvation effects were accounted for during structure optimizations using the COSMO solvation model with a dielectric constant of infinity.[57,58] Final solvation free energies were calculated for each structure at 25 °C using the COSMO-RS[59] model in COSMOTherm (version 2018) with the parameter file BP_TZVP_18.ctd based on BP86[60]/def-TZVP level. The Gibbs free energies in solution were then calculated from a thermodynamic cycle $G = E$ + c.p. + G_{solv}, where E is the gas-phase energy of the system at the RPA level, c.p. is the chemical potential based on standard rigid-rotor harmonic oscillator approximation at 25 °C, and G_{solv} is the free energy of solvation obtained from COSMO-RS. The thermodynamic reference state of the so-obtained free energies refers to a hypothetic mole fraction of 1 for all species, which were converted into a reference state of 1 mol/L using solvent molarities (c) of 9.41 and 12.3 mol/L for toluene and tetrahydrofuran, respectively, by adding a term $RT \ln(c)$ to the free energy of all species.

Initial structures that were used for structure optimizations correspond to the lowest energy conformer of each structure obtained from extensive conformational searches performed with respect to all rotatable bonds at the level of optimization without D3 correction. In the case of transition states, the forming and breaking bonds were constrained during the conformer search according to their initial guess structures, which were obtained using the single-ended growing string method.[61−63] Pictures of the computed structures were

https://doi.org/10.1021/acs.joc.1c00119
J. Org. Chem. 2021, 86, 5651−5659

generated using CYLview.[64] Cartesian coordinates of all optimized structures are included in the Supporting Information.

4.2. Experimental Details. Phenyl isocyanate (≥98%), *p*-tolyl isocyanate (≥99%), and cesium pivalate (≥98%) were purchased from Sigma-Aldrich; tetrabutylammonium acetate (>90%), triethylamine (>99%), and potassium 2-ethylhexanoate (>95%) were purchased from TCI. All of the reagents above were used directly without treatment. THF (without stabilizer BHT) was directly obtained from the dry solvent system; toluene was dried by mol-sieves before use; and pentane was directly used without treatment. Fourier-transform infrared spectroscopy (FTIR) measurements were carried out in the attenuated reflection mode on a Spectrum One (Perkin Elmer) spectrometer at room temperature. Eight scans were performed from 4000 to 450 cm^{-1}. Liquid chromatography−mass spectrometry (LC−MS) measurements were carried out on a LCQ Fleet ESI-MS (Thermo Fisher Scientific) with H_2O (0.1% formic acid) as eluents. As the intermediates are negatively charged, a negative−positive mode LC−MS was adapted, and water and the formic acid eluent were used to protonate the intermediates, which provided clear signals in the positive spectrum. The reaction mixtures were further analyzed identically for reactions done with phenyl and *p*-tolyl isocyanates to assist the identification of different intermediates in LC−MS spectra by indicating the number of aromatic groups present. NMR measurements for characterization of the compounds and identification of double bonds were performed using either a Bruker UltraShield 400 MHz or Varian Mercury 400 MHz spectrometer at room temperature using acetone-d_6 as a solvent.

4.3. Study of Cyclotrimerization Mechanism of Phenyl and *p*-Tolyl Isocyanates Using Carboxylates (TBAA, Potassium 2-Ethylhexanoate or Cesium Pivalate) as Catalysts. Phenyl isocyanate (0.53 g, 4.44 mmol) or *p*-tolyl isocyanate (0.52 g, 3.92 mmol) was dissolved in THF or toluene (5.0 mL) in a dry flask. The catalyst solution was prepared by dissolving the catalyst (10 mol % to NCO groups) in THF or toluene (5.5 mL) in a separate dry flask and then added to the isocyanate solution (concentration of phenyl isocyanate: 0.5 g/10 mL solvent). The reaction was carried out at room temperature for all catalysts except that a temperature of 60 °C in an oil bath was used for cesium pivalate (due to its poor solubility). All reactions were performed under an Ar atmosphere until the disappearance of NCO stretching vibration at 2270 cm^{-1} as observed by IR measurement. After that, most of the solvent was evaporated in an Ar flow. The so formed sample was diluted in water/acetonitrile (1:1) solution with a concentration of 1 mg/mL for LC−MS measurement and dissolved in acetone-d_6 for NMR measurement.

4.4. Study of Cyclotrimerization Mechanism of Phenyl Isocyanates Using Deprotonated Acetanilide as a Catalyst. Phenyl isocyanate (0.58 g, 4.85 mmol) was dissolved in THF or toluene (5.0 mL) in a dry flask. The catalyst solution was prepared by dissolving acetanilide (10 mol % to NCO groups) and triethylamine (30 mol % to NCO groups) in THF (6.6 mL) in a separate dry flask and then added to the isocyanate solution (concentration of phenyl isocyanate: 0.5 g/10 mL solvent). The reaction was carried out at room temperature under an Ar atmosphere overnight. After that, most of the solvent was blown by an Ar flow and wet precipitates were obtained. The sample was diluted in water/acetonitrile (1:1) solution with a concentration of 1 mg/mL for LC−MS measurement.

4.5. Synthesis and Purification of Tris-*p*-Tolyl Isocyanurate Using Potassium 2-Ethylhexanoate as a Catalyst. *p*-Tolyl isocyanate (1.15 g, 8.67 mmol) was dissolved in THF (3.0 mL) in a dry flask. The catalyst solution was prepared by dissolving potassium 2-ethylhexanoate (1 mol % to NCO groups) in THF (2.6 mL) in a separate dry flask and then added to the isocyanate solution. The reaction was carried out in a 40 °C oil bath under an Ar atmosphere until the disappearance of NCO stretching vibration at 2270 cm^{-1} as observed by IR measurement. After the reaction, 10 mL of THF was added to dissolve all of the precipitates at 40 °C. Then, the tris-*p*-tolyl isocyanuate was precipitated by direct pouring the warm solution in cooled pentane. The precipitate was immediately filtered and dried in a vacuum oven at 60 °C overnight, giving tris-*p*-tolyl isocyanurate as a white powder (0.96 g, 2.40 mmol, yield: 83%). ^1H NMR (400 MHz, acetone-d_6): δ 7.29 (t, J = 6.1 Hz, 12H), 2.36 (s, 9H) ppm; $^{13}C\{^1H\}$ NMR (100 MHz, acetone-d_6): δ 205.3, 129.4, 128.7, and 20.3 ppm.[65]

■ ASSOCIATED CONTENT

Supporting Information

The Supporting Information is available free of charge at https://pubs.acs.org/doi/10.1021/acs.joc.1c00119.

Cartesian coordinates of all optimized structures and computed energies, LC−MS, and NMR data for all mechanistic studies (PDF)

■ AUTHOR INFORMATION

Corresponding Authors

Mikko Muuronen − *BASF SE, 67056 Ludwigshafen am Rhein, Germany;* orcid.org/0000-0001-9647-7070; Email: mikko.muuronen@basf.com

Željko Tomović − *Polymer Performance Materials Group, Department of Chemical Engineering and Chemistry, Eindhoven University of Technology, 5600 MB Eindhoven, The Netherlands;* orcid.org/0000-0002-7944-5728; Email: z.tomovic@tue.nl

Authors

Yunfei Guo − *Polymer Performance Materials Group, Department of Chemical Engineering and Chemistry, Eindhoven University of Technology, 5600 MB Eindhoven, The Netherlands*

Peter Deglmann − *BASF SE, 67056 Ludwigshafen am Rhein, Germany*

Frederic Lucas − *BASF SE, 67056 Ludwigshafen am Rhein, Germany*

Rint P. Sijbesma − *Supramolecular Polymer Chemistry Group, Department of Chemical Engineering and Chemistry, Eindhoven University of Technology, 5600 MB Eindhoven, The Netherlands; Institute for Complex Molecular Systems, Eindhoven University of Technology, 5600 MB Eindhoven, The Netherlands;* orcid.org/0000-0002-8975-636X

Complete contact information is available at: https://pubs.acs.org/10.1021/acs.joc.1c00119

Author Contributions

⊥Y.G. and M.M. contributed equally.

Notes

The authors declare no competing financial interest.

■ ACKNOWLEDGMENTS

The authors would like to thank Dr. Xianwen Lou (TU Eindhoven) for discussions on LC−MS spectra and Dr. Rebecca Sure (BASF SE) for discussions on isocyanate trimerization mechanisms. The authors also acknowledge financial support from BASF Polyurethanes GmbH.

■ REFERENCES

(1) Engels, H. W.; Pirkl, H. G.; Albers, R.; Albach, R. W.; Krause, J.; Hoffmann, A.; Casselmann, H.; Dormish, J. Polyurethanes: Versatile Materials and Sustainable Problem Solvers for Today's Challenges. *Angew. Chem., Int. Ed.* **2013**, *52*, 9422−9441.

(2) Randall, D.; Lee, S. *The Polyurethanes Book*; Wiley, 2003.

(3) Eling, B.; Tomović, Ž.; Schädler, V. Current and Future Trends in Polyurethanes: An Industrial Perspective. *Macromol. Chem. Phys.* **2020**, *221*, No. 2000114.

(4) Delebecq, E.; Pascault, J. P.; Boutevin, B.; Ganachaud, F. On the Versatility of Urethane/Urea Bonds: Reversibility, Blocked Isocya-

nate, and Non-Isocyanate Polyurethane. *Chem. Rev.* **2013**, *113*, 80−118.
(5) Wang, G.; Li, K.; Zou, W.; Hu, A.; Hu, C.; Zhu, Y.; Chen, C.; Guo, G.; Yang, A.; Drumright, R.; Argyropoulos, J. Synthesis of ADI/HDI Hybrid Isocyanurate and Its Application in Polyurethane Coating. *J. Coat. Technol. Res.* **2015**, *12*, 543−553.
(6) Driest, P. J.; Lenzi, V.; Marques, L. S. A.; Ramos, M. M. D.; Dijkstra, D. J.; Richter, F. U.; Stamatialis, D.; Grijpma, D. W. Aliphatic Isocyanurates and Polyisocyanurate Networks. *Polym. Adv. Technol.* **2017**, *28*, 1299−1304.
(7) Laas, H. J.; Halpaap, R.; Pedain, J. Zur Synthese Aliphatischer Polyisocyanate − Lackpolyisocyanate Mit Biuret-, Isocyanurat- Oder Uretdionstruktur. *J. Prakt. Chem./Chem.-Ztg.* **1994**, *336*, 185−200.
(8) Meier-Westhues, H.-U. et al. *Polyurethanes: Coatings, Adhesives and Sealants*; European Coatings, 2019.
(9) Kordomenos, P. I.; Kresta, J. E. Thermal Stability of Isocyanate-Based Polymers. 1. Kinetics of the Thermal Dissociation of Urethane, Oxazolidone, and Isocyanurate Groups. *Macromolecules* **1981**, *14*, 1434−1437.
(10) Kordomenos, P. I.; Kresta, J. E.; Frisch, K. C. Thermal Stability of Isocyanate-Based Polymers. 2. Kinetics of the Thermal Dissociation of Model Urethane, Oxazolidone, and Isocyanurate Block Copolymers. *Macromolecules* **1987**, *20*, 2077−2083.
(11) Reymore, H. E.; Carleton, P. S.; Kolakowski, R. A.; Sayigh, A. A. R. Isocyanu Rate Foams: Chemistry, Properties and Processing. *J. Cell. Plast.* **1975**, *11*, 328−344.
(12) Wang, C. L.; Klempner, D.; Frisch, K. C. Morphology of Polyurethane- Isocyanurate Elastomers. *J. Appl. Polym. Sci.* **1985**, *30*, 4337−4344.
(13) Kogon, I. C. New Reactions of Phenyl Isocyanate and Ethyl Alcohol. *J. Am. Chem. Soc.* **1956**, *78*, 4911−4914.
(14) Duff, D. W.; Maciel, G. E. Monitoring the Thermal Degradation of an Isocyanurate-Rich MDI-Based Resin by ^{15}N and ^{13}C CP/MAS NMR. *Macromolecules* **1991**, *24*, 651−658.
(15) Chattopadhyay, D. K.; Webster, D. C. Thermal Stability and Flame Retardancy of Polyurethanes. *Prog. Polym. Sci.* **2009**, *34*, 1068−1133.
(16) Xu, Q.; Hong, T.; Zhou, Z.; Gao, J.; Xue, L. The Effect of the Trimerization Catalyst on the Thermal Stability and the Fire Performance of the Polyisocyanurate-Polyurethane Foam. *Fire Mater.* **2018**, *42*, 119−127.
(17) Dick, C.; Dominguez-Rosado, E.; Eling, B.; Liggat, J. J.; Lindsay, C. I.; Martin, S. C.; Mohammed, M. H.; Seeley, G.; Snape, C. E. The Flammability of Urethane-Modified Polyisocyanurates and Its Relationship to Thermal Degradation Chemistry. *Polymer* **2001**, *42*, 913−923.
(18) Jozef, B. G.; Eric, H.; Stijn, R.; Marc, V.; Guido, V. H. G. Process for Preparing a Polyisocyanurate Polyurethane Material. U.S. Patent US2008/0283851A12008.
(19) Al Nabulsi, A.; Cozzula, D.; Hagen, T.; Leitner, W.; Müller, T. E. Isocyanurate Formation during Rigid Polyurethane Foam Assembly: A Mechanistic Study Based on: In Situ IR and NMR Spectroscopy. *Polym. Chem.* **2018**, *9*, 4891−4899.
(20) Hagquist, J. A. E.; Reid, K. J.; Giorgini, A.; Hill, N. Isocyanurate Embedment Compound. U.S. Patent US5556934A1996.
(21) Burdeniuc, J. J.; Panitzsch, T.; Dewhurst, J. E. Trimerization Catalysts from Sterically Hindered Salts. U.S. Patent US8530534B22013.
(22) Bechara, I. Some Aspects of Innovative Catalysis of the Isocyanate Trimerization Reaction − Polyisocyanurate Foam Formation and Properties. *J. Cell. Plast.* **1979**, *15*, 102−113.
(23) Driest, P. J.; Dijkstra, D. J.; Stamatialis, D.; Grijpma, D. W. The Trimerization of Isocyanate-Functionalized Prepolymers: An Effective Method for Synthesizing Well-Defined Polymer Networks. *Macromol. Rapid Commun.* **2019**, *40*, No. 1800867.
(24) Driest, P. J.; Dijkstra, D. J.; Stamatialis, D.; Grijpma, D. W. Tough Combinatorial Poly(Urethane-Isocyanurate) Polymer Networks and Hydrogels Synthesized by the Trimerization of Mixtures of NCO-Prepolymers. *Acta Biomater.* **2020**, *105*, 87−96.
(25) Achten, D.; Matner, M.; Casselmann, H.; Ehlers, M. Polyisocyanurate Plastics Having High Thermal Stability. WIPO Patent WO2016/1700612018.
(26) Nambu, Y.; Endo, T. Synthesis of Novel Aromatic Isocyanurates by the Fluoride-Catalyzed Selective Trimerization of Isocyanates. *J. Org. Chem.* **1993**, *58*, 1932−1934.
(27) Heift, D.; Benko, Z.; Grützmacher, H.; Jupp, A. R.; Goicoechea, J. M. Cyclo-Oligomerization of Isocyanates with Na(PH2) or Na(OCP) as "p-" Anion Sources. *Chem. Sci.* **2015**, *6*, 4017−4024.
(28) Moghaddam, F. M.; Dekamin, M. G.; Khajavi, M. S.; Jalili, S. Efficient and Selective Trimerization of Aryl and Alkyl Isocyanates Catalyzed by Sodium P-Toluenesulfinate in the Presence of TBAI in a Solvent-Free Condition. *Bull. Chem. Soc. Jpn.* **2002**, *75*, 851−852.
(29) Moritsugu, M.; Sudo, A.; Endo, T. Development of High-Performance Networked Polymers Consisting of Isocyanurate Structures Based on Selective Cyclotrimerization of Isocyanates. *J. Polym. Sci., Part A: Polym. Chem.* **2011**, *49*, 5186−5191.
(30) Giuglio-Tonolo, A. G.; Spitz, C.; Terme, T.; Vanelle, P. An Expeditious Method for the Selective Cyclotrimerization of Isocyanates Initiated by TDAE. *Tetrahedron Lett.* **2014**, *55*, 2700−2702.
(31) Tang, J.; Mohan, T.; Verkade, J. G. Selective and Efficient Syntheses of Perhydro-1,3,5-Triazine-2,4,6-Triones and Carbodiimides from Isocyanates Using ZP(MeNCH2CH2)3N Catalysts. *J. Org. Chem.* **1994**, *59*, 4931−4938.
(32) Gibb, J. N.; Goodman, J. M. The Formation of High-Purity Isocyanurate through Proazaphosphatrane- Catalysed Isocyanate Cyclo-Trimerisation: Computational Insights. *Org. Biomol. Chem.* **2013**, *11*, 90−97.
(33) Raders, S. M.; Verkade, J. G. An Electron-Rich Proazaphosphatrane for Isocyanate Trimerization to Isocyanurates. *J. Org. Chem.* **2010**, *75*, 5308−5311.
(34) Li, C.; Zhao, W.; He, J.; Zhang, Y. Highly Efficient Cyclotrimerization of Isocyanates Using N-Heterocyclic Olefins under Bulk Conditions. *Chem. Commun.* **2019**, *55*, 12563−12566.
(35) Duong, H. A.; Cross, M. J.; Louie, J. N-Heterocyclic Carbenes as Highly Efficient Catalysts for the Cyclotrimerization of Isocyanates. *Org. Lett.* **2004**, *6*, 4679−4681.
(36) Duff, D. W.; Maciel, G. E. 13C and 15N CP/MAS NMR Characterization of MDI-Polyisocyanurate Resin Systems. *Macromolecules* **1990**, *23*, 3069−3079.
(37) Silva, A. L.; Bordado, J. C. Recent Developments in Polyurethane Catalysis: Catalytic Mechanisms Review. *Catal. Rev.* **2004**, *46*, 31−51.
(38) Krestra, J. E. Reaction Injection Molding and Fast Polymerization Reactions. In *Polymer Science and Technology*; Springer, 1982; Vol. *18*, pp 147−168.
(39) Hoffman, D. K. Model System for a Urethane-Modified Isocyanurate Foam. *J. Cell. Plast.* **1984**, *20*, 129−137.
(40) Schwetlick, K.; Noack, R. Kinetics and Catalysis of Consecutive Isocyanate Reactions. Formation of Carbamates, Allophanates and Lsocyanurates. *J. Chem. Soc., Perkin Trans. 2* **1995**, 395−402.
(41) Siebert, M.; Sure, R.; Deglmann, P.; Closs, A. C.; Lucas, F.; Trapp, O. Mechanistic Investigation into the Acetate-Initiated Catalytic Trimerization of Aliphatic Isocyanates: A Bicyclic Ride. *J. Org. Chem.* **2020**, *85*, 8553−8562.
(42) Tao, J.; Perdew, J.; Staroverov, V.; Scuseria, G. Climbing the Density Functional Ladder: Nonempirical Meta-Generalized Gradient Approximation Designed for Molecules and Solids. *Phys. Rev. Lett.* **2003**, *91*, No. 146401.
(43) Grimme, S.; Antony, J.; Ehrlich, S.; Krieg, H. A Consistent and Accurate Ab Initio Parametrization of Density Functional Dispersion Correction (DFT-D) for the 94 Elements H-Pu. *J. Chem. Phys.* **2010**, *132*, No. 154104.
(44) Weigend, F.; Furche, F.; Ahlrichs, R. Gaussian Basis Sets of Quadruple Zeta Valence Quality for Atoms H-Kr. *J. Chem. Phys.* **2003**, *119*, 12753.
(45) Weigend, F.; Ahlrichs, R. Balanced Basis Sets of Split Valence, Triple Zeta Valence and Quadruple Zeta Valence Quality for H to Rn:

https://doi.org/10.1021/acs.joc.1c00119
J. Org. Chem. 2021, 86, 5651−5659

Design and Assessment of Accuracy. *Phys. Chem. Chem. Phys.* **2005**, *7*, 3297.
(46) Eshuis, H.; Yarkony, J.; Furche, F. Fast Computation of Molecular Random Phase Approximation Correlation Energies Using Resolution of the Identity and Imaginary Frequency Integration. *J. Chem. Phys.* **2010**, *132*, No. 234114.
(47) Muuronen, M.; Deglmann, P.; Tomović, Ž. Design Principles for Rational Polyurethane Catalyst Development. *J. Org. Chem.* **2019**, *84*, 8202−8209.
(48) Nguyen, B. D.; Chen, G. P.; Agee, M. M.; Burow, A. M.; Tang, M. P.; Furche, F. Divergence of Many-Body Perturbation Theory for Noncovalent Interactions of Large Molecules. *J. Chem. Theory Comput.* **2020**, *16*, 2258−2273.
(49) Grimme, S. Supramolecular Binding Thermodynamics by Dispersion-Corrected Density Functional Theory. *Chem. − Eur. J.* **2012**, *18*, 9955−9964.
(50) Mader, P. M. Hydrolysis Kinetics for P-Dimethylaminophenyl Isocyanate in Aqueous Solutions. *J. Org. Chem.* **1968**, *33*, 2253−2260.
(51) Lenzi, V.; Driest, P. J.; Dijkstra, D. J.; Ramos, M. M. D.; Marques, L. S. A. Investigation on the Intermolecular Interactions in Aliphatic Isocyanurate Liquids: Revealing the Importance of Dispersion. *J. Mol. Liq.* **2019**, *280*, 25−33.
(52) Balasubramani, S. G.; Chen, G. P.; Coriani, S.; Diedenhofen, M.; Frank, M. S.; Franzke, Y. J.; Furche, F.; Grotjahn, R.; Harding, M. E.; Hättig, C.; Hellweg, A.; Helmich-Paris, B.; Holzer, C.; Huniar, U.; Kaupp, M.; Khah, A. M.; Khani, S. K.; Müller, T.; Mack, F.; Nguyen, B. D.; Parker, S. M.; Perlt, E.; Rappoport, D.; Reiter, K.; Roy, S.; Rückert, M.; Schmitz, G.; Sierka, M.; Tapavicza, E.; Tew, D. P.; Wüllen, C.; van Voora, V. K.; Weigend, F.; Wodyński, A.; Yu, J. M. TURBOMOLE: Modular Program Suite for Ab Initio Quantum-Chemical and Condensed-Matter Simulations. *J. Chem. Phys.* **2020**, *152*, No. 184107.
(53) Sierka, M.; Hogekamp, A.; Ahlrichs, R. Fast Evaluation of the Coulomb Potential for Electron Densities Using Multipole Accelerated Resolution of Identity Approximation. *J. Chem. Phys.* **2003**, *118*, 9136−9148.
(54) Weigend, F. Accurate Coulomb-Fitting Basis Sets for H to Rn. *Phys. Chem. Chem. Phys.* **2006**, *8*, 1057−1065.
(55) Weigend, F.; Häser, M.; Patzelt, H.; Ahlrichs, R. RI-Mp2: Optimized Auxiliary Basis Sets and Demonstration of Efficiency. *Chem. Phys. Lett.* **1998**, *294*, 143.
(56) Hättig, C. Optimization of Auxiliary Basis Sets for RI-MP2 and RI-CC2 Calculations: Core−Valence and Quintuple-ζ Basis Sets for H to Ar and QZVPP Basis Sets for Li to Kr. *Phys. Chem. Chem. Phys.* **2005**, *7*, 59.
(57) Schäfer, A.; Klamt, A.; Sattel, D.; Lohrenz, J. C. W.; Eckert, F. COSMO Implementation in TURBOMOLE: Extension of an Efficient Quantum Chemical Code towards Liquid Systems. *Phys. Chem. Chem. Phys.* **2000**, *2*, 2187−2193.
(58) Klamt, A.; Schueuermann, G. COSMO: A New Approach to Dielectric Screening in Solvents with Explicit Expressions for the Screening Energy and Its Gradient. *J. Chem. Soc., Perkin Trans. 2* **1993**, 799−805.
(59) Klamt, A.; Eckert, F. COSMO-RS: A Novel and Efficient Method for the a Priori Prediction of Thermophysical Data of Liquids. *Fluid Phase Equilib.* **2000**, *172*, 43−72.
(60) Becke, A. D. Density-Functional Exchange-Energy Approximation with Correct Asymptotic Behavior. *Phys. Rev. A* **1988**, *38*, No. 3098.
(61) Zimmerman, P. Reliable Transition State Searches Integrated with the Growing String Method. *J. Chem. Theory Comput.* **2013**, *9*, 3043−3050.
(62) Zimmerman, P. M. Growing String Method with Interpolation and Optimization in Internal Coordinates: Method and Examples. *J. Chem. Phys.* **2013**, *138*, No. 184102.
(63) Zimmerman, P. M. Single-Ended Transition State Finding with the Growing String Method. *J. Comput. Chem.* **2015**, *36*, 601−611.
(64) Legault, C. Y. *CYLview*; Université de Sherbrooke, 2009. http://www.cylview.org.
(65) Bahili, M. A.; Stokes, E. C.; Amesbury, R. C.; Ould, D. M. C.; Christo, B.; Horne, R. J.; Kariuki, B. M.; Stewart, J. A.; Taylor, R. L.; Williams, P. A.; Jones, M. D.; Harris, K. D. M.; Ward, B. D. Aluminium-Catalysed Isocyanate Trimerization, Enhanced by Exploiting a Dynamic Coordination Sphere. *Chem. Commun.* **2019**, *55*, 7679−7682.

https://doi.org/10.1021/acs.joc.1c00119
J. Org. Chem. 2021, 86, 5651−5659